The Numerical Simulation of a Subtractive Process for the Fabrication of 3D Low Temperature Co-Fired Ceramics Packaging Structures and Devices: Jet Vapor Etching

Idalia Ramos #, Laiza García #, Eliphas Wagner Simoes ∗, Rogerio Furlan # ∗, J.J. Santiago-Aviles ∗ +,
and Marcos Tadeu Pereira++

University of Puerto Rico at Humacao, Department of Physics and Electronics, Humacao, PR
∗Laboratorio de Sistemas Integraveis, Escola Politecnica da Universidade de Sao Paulo, SP, Brazil
+ University of Pennsylvania, Department of Electrical Engineering, Philadelphia, PA, USA.
++ Laboratorio de Vazão, Instituto de Pesquisas Tecnologicas, Sao Paulo, SP, Brazil

CUH Station, Humacao, PR, 00791, tel: 787-850-9381, , fax: 787-850-9308
e-mail: iramos@cuhwww.upr.clu.edu, laiza_0904@hotmail.com, eliphas@lsi.usp.br,
r_furlan@cuhac.upr.clu.edu, santiago@ee.upenn.edu, and marcostp@ipt.br

ABSTRACT

We applied numerical simulation in order to gain knowledge and insight into the physical processes associated with Jet Vapor Etching, a subtractive process used in the machining of Low Temperature Co-Fired Ceramic (LTCC) tapes. Also, we performed a series of time independent (steady state) simulations of the process reactor, dividing the reactor in three parts and using the results of each part as to define the boundary conditions of the subsequent part. Furthermore we explore the dependence of the machined feature size on the pressure, temperature, distance from the micro-machined silicon nozzle to the LTCC tape, and nozzle geometry. We display velocity vector as well as density gradient profiles combined with distance dependence to substantiate the argument in our narrative.

Keywords: jet vapor etching, nozzle, green tape, fluid mechanics, and simulation

1 INTRODUCTION

Low Temperature Co-Fired Ceramics (LTCC) [1], also called green ceramic tapes, because they are manipulated at the green stage before firing and sintering, is an important material for meso and micro-scale applications. The typical material is a glass – ceramic composite containing ceramic filler, usually alumina (Al_2O_3), and the binder a lead, aluminum, and silica glass. It also includes an organic binder (plasticizer plus anti - flocculant). Among the multiple advantages of using LTCC we can mention the following: 3D structures can be fabricated using multiple layers, wide range of properties could be achieved by modifying the filler, it can be integrated with a variety of other materials. In addition, its mechanical and thermal properties can be modified by the use of vias.

Jet Vapor Etching (*JVE*) of LTCC [2] is a process that consists on locally dissolving the organic binder on the tape using atomized acetone transported by a nitrogen carrier. Figure 1 displays the schematics of a *JVE* reactor. The momentum of the mixture removes the glass and alumina grains. Jet Vapor Etching has as one of its main features the possibility of fast prototyping, as it allows direct definition of the etched pattern in a few hours. There is no mask fabrication involved, no lamination of resist, and no pre-processing (partially sintering) of the tape. With this method we were able to obtain the smallest via size in LTCC (~10 μm of diameter). To achieve this, an XYZ computer station dwells and moves the green tape. This movement defines the pattern to be transferred. This technique is somewhat similar to the so-called additive techniques for rapid prototyping (deposition of layers upon layers), except we do the opposite, removing material. So it is indeed a subtractive manufacturing technique.

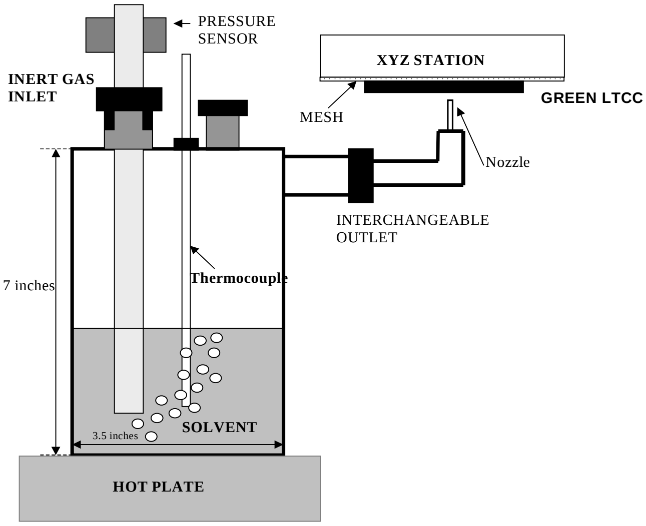

Figure 1: Jet Vapor Etching reactor.

This process is simple and can be easily accommodated in a standard LTCC facility. We have found that the solvent vapor jet impinging on the ceramic tape sample can produce cavities with variable morphologies depending on the processing conditions, such as carrier pressure, outlet pressure, ceramic tape temperature and distance from nozzle tip to the ceramic tape surface and ceramic tape feed rate.

We are currently simulating the reactor using the ANSYS/FLOTRAN 5.7 commercial simulation package as a whole by dividing it in three parts. The first part consists of the vessel and the carrier gas manifold. The second part is the outlet channel, from the cylindrical vessel to the tip, where the nozzle lies, and the third part is the nozzle itself and its surroundings. The advantage of analyzing the reactor in three parts is that one can use the solution of one part as a means of obtaining reasonable boundary conditions for the subsequent part as one goes from carrier gas inlet to jet outlet.

2 SIMULATIONS PROCEDURES

Many of the simulations presented in the literature use the ANSYS finite-element program - which has a specific module (or library) for steady state or transient simulations in fluids, denominated FLOTRAN [3]. We wish to emphasize that in order to simplify the computational process, we assumed that due to its cylindrical symmetry, a two-dimensional analysis would be adequate to test the Jet Vapor Etching apparatus. In this case, we are using the simulations to obtain an overview of possible conditions inside each part of the reactor. Furthermore, to determine the shape of downstream jet output of the silicon nozzle (typical hydraulic diameter of 50; 150; 220; and 250 μm with distance between silicon nozzle from green tape of 660; 1320; and 1980 μm) and to compare the simulation with obtained experimental results. The basic vessel and the carrier gas manifold is simulated using the FLOTRAN 141, the element of ANSYS for two-dimensional analysis. In this case, this structure defined a total of 5432 nodes.

The silicon nozzle morphology corresponds to a typical shape obtained using the KOH chemical wet etching as indicated in Figure 2. The open window in the backside of the silicon chip (parameter L) can be obtained using the expression (1), as a function of nozzle width (d) and silicon wafer thickness (e), these values are indicated in Table 1.

$$L = 2.e.\text{cotg}\,(57.4°) + d \qquad (1)$$

Figure 3 shows the silicon nozzle (in this case with a hydraulic diameter of the 150 μm) and the green tape position (i.e. 660 μm to silicon nozzle output) using the same element indicated above and 2451 nodes. Observe, how this very simple procedure allow us to minimize the problems associated with the mesh configuration and to reduce significantly the aspect ratio variation for the two-dimensional element used for mapping each part of the reactor.

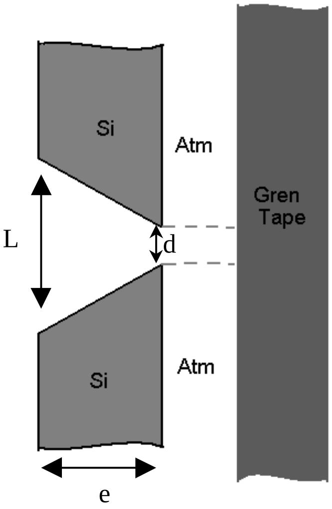

Figure 2: Typical nozzle geometry obtained using KOH anisotropic etching.

Table 1: Geometrical parameter of silicon nozzles:

e (μm)	d (μm)	L (μm)
300	50	433
300	150	533
300	220	603
300	250	633

We found this configuration suitable in terms of our computational resources utilization (PC platform with a Pentium III, 750 MHz, and 512 MB of RAM) and simulation time. We used standard two-equation κ–ε turbulent models and FLOTRAN 141 elements (rectangular form, 4 nodes, and 2D space).

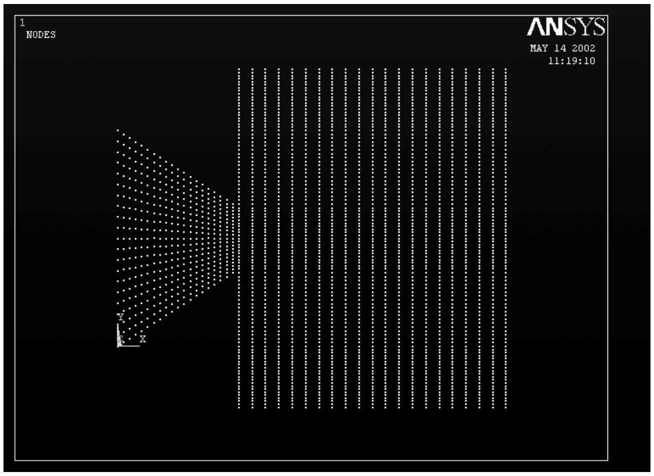

Figure 3: Silicon nozzle to green tape configuration defined using 2451 nodes.

A minimum of 1500 iterations steady state analysis was necessary to obtain the desired convergence for the results. A value lower than 10^{-5} was adopted for the convergence criteria, calculated as E, in expression 2:

$$E = \sum_{i=1}^{N} \frac{| \phi i_i^k - \phi i_i^{k-1} |}{| \phi i_i^k |} \qquad (2)$$

Where ϕ is a degree of freedom (pressure, velocity, temperature, etc.), N is the total number of nodes, i is the iteration number and k is the number of iterations.

The internal flow (velocity) behavior was analyzed as a function of the relative supply pressure, considering values between 41.368 kPa to 82.737 kPa, which lead to reasonable velocity. The relative external pressures were assumed to be slightly higher than the reference pressure (~100 Pa). The reference pressure was assumed to be 101.35 kPa. The physical parameters (density (ρ), viscosity (μ), etc.) employed were those of Nitrogen (N_2) and Acetone (C_3H_6O) vapor.

3 RESULTS AND DISCUSSION

The relatively quick entry into non-linear behavior (Figure 4) shown by the feature diameter as a function of nozzle width and shown by the simulation results may provide us with an extended dynamic range in terms of LTCC fabrication. A great deal of latitude in the feature diameter can be obtained by just changing the nozzle diameter a few times. One can achieve an increment of over 500 µm in the feature diameter by varying the nozzle size by a mere 100 µm, at a constant distance from the LTCC tape.

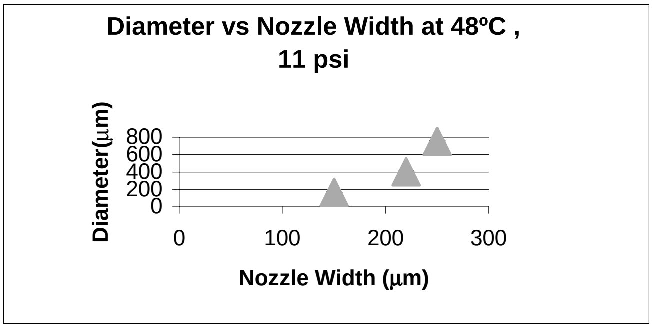

Figure 4: Fabricated feature diameter as a function of the nozzle diameter. Note the exponential like behavior .

The results of the simulations show that the velocity vector profile for small nozzles (less than 220 µm, see Figure 5 for a 150 µm nozzle) are usually laminar, subsonic and transonic with the usual cigar shape. Once we reach a diameter of 250 µm, the Reynolds number show that even for nitrogen gas, we are most likely in a turbulent regime (Re>5500).

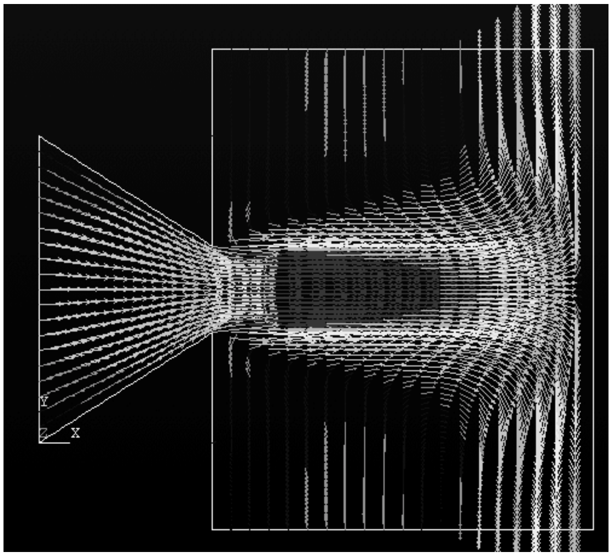

Figure 5: Simulated velocity vector profile, note cigar shape and symmetry.

The most striking feature of the density profile for the small diameter nozzle is the high density along the axis and in proximity to the target. It most likely the result of the jet "bouncing" on the target LTCC tape and reinforcing the intensity of the density false gray tone map. This density maximum might interfere with the particle flux leaving the target LTCC tape upon being expelled by the binder dissolution. This phenomenon, see Figure 6, might merit further simulation and experimental work, as it is quite relevant to the manufacturing application.

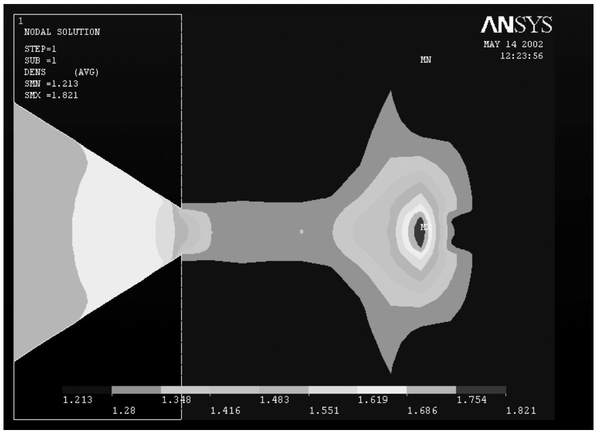

Figure 6: Simulated densities profile (in Kg/m^3), note the "bouncing" effect when the flow strikes the target LTCC tape.

Figure 7 clearly shows the formation of eddies with a minimal velocity front where the symmetry axis cut the target. Note a maximum (or nearly so) at a total distance of nearly one mm for a feature to nozzle diameter ratio of about 3 or 4, a fact readily observed in the experiments.

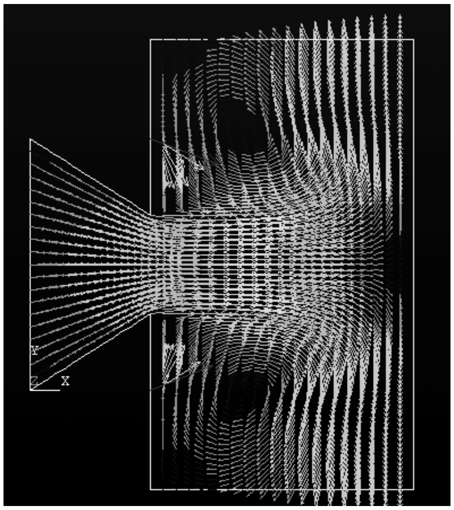

Figure 7: Velocity vector profiles for a 250 μm nozzle diameter.

From the density profiles shown in Figure 8 one can note the fact that the density tends to be higher where the axis cut the target LTCC. The momentum being proportional to the product of the density and velocity might justify our claim that momentum transfer might be the likely mechanism for the removal of the filler particles once the binder disappear. Of course the vortices will also help in the particle transport.

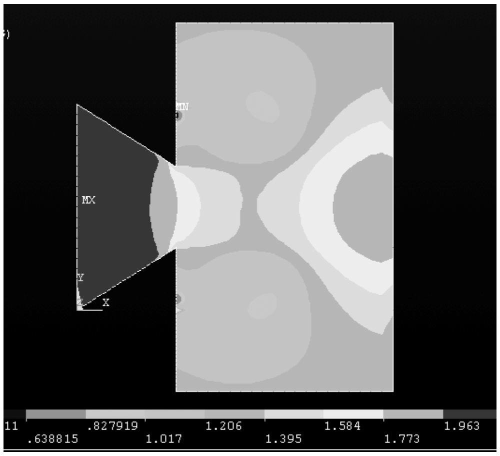

Figure 8: Gas density profiles (in Kg/m^3) under the same conditions above.

Figure 9 shows the distance dependence of the density profile. In part (a) the nozzle to target distance is 660 μm and in part (b) is 1320 μm. Note that the density maximum lies in the symmetry axis next to the target, independent of the distance, a bit of a flow focus effect but the nearer the target the larger the density and the faster the binder removal. The radial density gradient implies a soft boundary in the removal process and a sidewall not perpendicular to the LTCC tape basal plane.

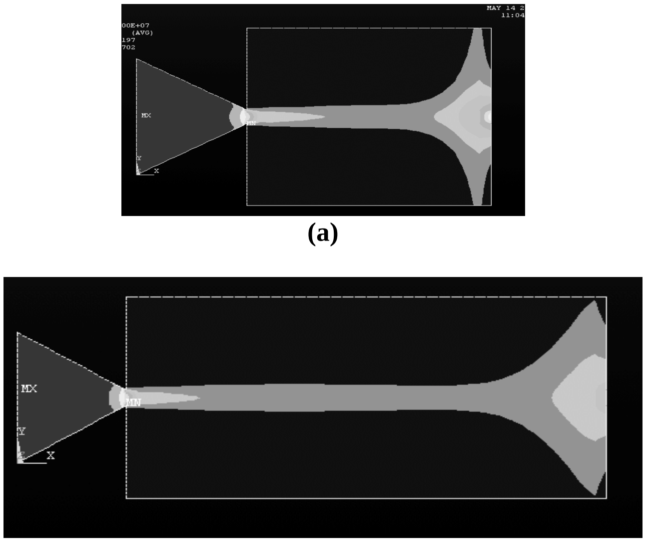

(a)

(b)

Figure 9: Density profiles showing dependence on distance from nozzle to LTCC target for a 50 μm nozzle. Note that for figure (b) the target is twice as far as for (a).

CONCLUSIONS

After the simulations exercise, it is reasonably clear that the results obtained not only reproduce qualitatively the experimental results obtained so far, but it gave us a good quantitative perspective on the process of Jet Vapor Etching. The various simulations also provided us with insight into the physical phenomena and ideas on how to modify and optimize the process.

Finally, the results obtained by simulation will be calibrated with the actual processing parameters. Carefully placing temperature sensors (thermocouples) and silicon micro-machined pressure transducers will allow us to obtain these local measurements. The ultimate purpose is to obtain a better quantitative outlook of the process.

ACKNOWLEDGEMENTS

The authors would like to acknowledge the financial support of NSF-DMR-9872689, FAPESP (Proc. Number 00/04218-0), PADCT and CNPq.

REFERENCES

[1] M.R. Gongora-Rubio, P. Espinoza-Vallejos, L. Sola-Laguna, J.J. Santiago-Aviles, Sensors and Actuators A 89, pp 222-241, 2001.

[2] P. Espinoza, J.F. Ortiz, I. Ramos, J.J. Santiago-Aviles, Proceedings of ICCCE/8, Tenerife, CI, pp 223-24, 2001.

[3] E. W. Simões, R. Furlan, and J. N. Zemel, Proceedings of the International Conference on Modeling and Simulation of Mycrosystems Semiconductors, pp. 480 – 485, 1998.